

Coil architectures for optical fiber rotation sensing

André C. Da Silva, Renato C. Rabelo, Ricardo T. De Carvalho, James N. Blake⁽¹⁾

*Instituto de Estudos Avançados (IEAv/CTA)
C. P. 6044, CEP 12231-970, São José dos Campos, SP, Brazil*

⁽¹⁾ *Texas A&M University (USA)*

Recebido 30 de junho 1998

An analysis is made of several different coil architectures available to assembly the fiber loop of a fiber optic gyroscope, including straight winding, dipole, quadrupole, octupole, and many others. For each number of layers from 1 to 32, a suitable architecture is proposed to minimize the pointing error due to both radial and longitudinal linear gradients of the refractive index induced by environmental perturbations. Sensitivities to winding errors are determined. A programmable machine capable of winding the fiber with a very low tension in any of the proposed architectures is conceived, assembled, and used to build a 10 cm diameter coil with 1 km of polarization maintaining fiber.

São analisadas diversas arquiteturas diferentes para a montagem de uma bobina de fibra óptica para um giroscópio, incluindo o enrolamento direto, o dipolar, o quadripolar, o octopolar e outros. Para cada número de camadas de 1 a 32, uma arquitetura adequada é proposta para minimizar o erro no ângulo devido a gradientes lineares no índice de refração, tanto radiais quanto longitudinais, induzidos por perturbações ambientais. Sensibilidades a erros de enrolamento são determinadas. Uma máquina programável capaz de bobinar a fibra com tensão baixa em qualquer uma das arquiteturas propostas é concebida, montada e utilizada para construir uma bobina com 10 cm de diâmetro e 1 km de fibra mantenedora de polarização.

I Introduction

The heart of the interferometric fiber optic gyroscope [1, 2] is a single mode optical fiber coil, where light is guided to manifest the Sagnac effect [2, 7]. This coil should be wound in a well engineered architecture for high sensitivity to inertial rotation [3] and very low sensitivity to any other environmental perturbation, such as thermal and mechanical fluctuations, vibration and acoustic waves. The research for satisfactory design solutions for this coil belongs the emerging science of optoelectronic packaging [4], as well as mechanical and product engineering.

The accuracy of a fiber optic gyroscope, ultimately limited by shot noise at the photodetector, is in practice limited by reciprocity noise, especially time-varying, environment-induced nonreciprocities [5, 6]. A local thermal fluctuation in the fiber, offset from the center of the coil, for example, causes a refractive index change and thus affects the counterpropagating waves

at different times. A differential phase shift will result and look like a rotation at the interferometer output. These errors can be substantially reduced by a suitable winding of the fiber coil, and different winding architectures have been devised to accomplish this task [6]. In this work, these and several alternative architectures are studied and compared.

II Background

Optical waves propagating in opposite directions in a Sagnac rotating fiber interferometer cumulate a non-reciprocal phase shift s proportional to the velocity of rotation Ω , given by [2, 7]:

$$s = \frac{4k_0 A \Omega}{c_0}, \quad (1)$$

where k_0 is the optical wavenumber, A is the area enclosed by the loop and c_0 is the speed of light in vacuum. Conversely, if a nonreciprocal phase shift due to

time-dependent perturbations is induced, it is usually indistinguishable from the Sagnac phase and yields an apparent rotation given by the same relation [5]. This happens because a perturbation in the propagation constant $\beta(l, t)$ at a given point l along the fiber affects the two beam at different times due to the finite speed of light. The resulting apparent rotation is a rate error given by [6]:

$$\Omega_E = \frac{d\theta_E}{dt} = \frac{c_0}{4k_0A}(s^+ - s^-), \quad (2)$$

where

$$s^+ = \int_0^L \beta(l, t - (L - l)/c) dl, \quad (3a)$$

$$s^- = \int_0^L \beta(l, t - l/c) dl, \quad (3b)$$

are the phase cumulated by each wave, $c = c_0/n_0$ their average phase velocity, assumed constant along coordinate l , n_0 the effective index of the guided modes, and L the total length of the fiber. Time integrals of rate errors lead to pointing errors (θ_E). Substitution of (3) into (2) and integration over a time greater than the transit time n_0L/c_0 yields

$$\theta_E = \frac{c_0}{4k_0A} \int_0^L \int_{t-l/c}^{t-(L-l)/c} \beta(l, t') dt' dl. \quad (4)$$

The pointing error builds up on an uninterrupted integration of infinitesimal rate errors as the perturbation occurs. When the perturbation stops and β becomes static, there is no instantaneous rate error, but the pointing error does not reset to zero and keeps constant, due to previous rate errors. In this situation, when $\beta(l, t) = \beta_0 + k_0 n(l)$, where $n(l)$ is the final value of the effective index due to a perturbation that took place after the gyro start-up time, (4) reduces to

$$\theta_E = \frac{n_0}{2A} \int_0^L (l - L/2) n(l) dl. \quad (5)$$

This is the figure of merit to be used in evaluating coil architectures. If $n(l)$ is symmetric around the center of the fiber, the integral in (5) is zero. For a given spatial index distribution $n(\mathbf{r})$, an architecture is to be found to make $n(l)$ be as symmetric as possible to minimize (5).

When a fiber with tension is wound on a rigid drum for several layers, inner layers are subject to a pressure analogous to the hydrostatic pressure, which increases linearly with depth. Heat diffusion from the inner to the outer layers also causes a linear radial distribution

of temperature. Since the refractive index change is proportional to both pressure and temperature, it is advisable to examine how the pointing error is affected by a spatial index perturbation with a linear gradient. The spatial index change considered is thus given by:

$$n(\mathbf{r}) = n_0 + n_r \frac{r - R_1}{R_N - R_1} + n_z \frac{z}{z_0}, \quad (6)$$

where n_r is the total index change from the first (inner, with radius R_1) to the last (outer, with radius R_N) layer, n_z is the total index change from the base ($z = 0$) to the top ($z = z_0$) fiber turns of the layer, and r and z are cylindrical coordinates.

III Coil architectures

A fiber of total length L and diameter D is coiled on a cylindrical drum of length l_D and diameter d_D usually with several layers and several turns in a layer. A layer of this coil is the fiber wound in such a geometry as to emulate a helical curve with a constant radius and a given longitudinal pitch between turns, wrapping an inner layer also with constant radius and longitudinal pitch. The step from one to the next outer layer is referred to as a radial pitch. The fiber will fill a torus of rectangular cross section. The gaps between turns and layers are filled with acrylate or some other material thermally and mechanically compatible with the fiber jacket. The i -th layer of the coil wraps a length of fiber L_i , in a total number of turns t_i , with radius R_i and a longitudinal pitch between turns p_i , assumed constant within the layer. A geometric relationship between these variables holds:

$$L_i = 2\pi T_i \sqrt{R_i^2 + p_i^2}, \quad (7)$$

where the radius R_i is given by

$$R_i = R_1 + \sum_{k=1}^{i-1} q_k, \quad (8)$$

q_k being the radial step between layers k and $k + 1$ and $R_1 = (d_D + D)/2$ the radius of the first (inner) layer. Usually the longitudinal pitch of the first layer p_1 is made equal to fiber diameter D , for maximum compactness. A coil with N layers encloses an area of

$$A = \sum_{i=1}^N (\pi R_i^2 t_i). \quad (9)$$

From Equations (7-9), used for computation of the pointing error given by (5), the independent variables

in the process of winding the fiber are the set $\{t_i, p_i, q_i\}$, $i = 1, 2N$. Once a coil architecture is defined to minimize the pointing error, the sensitivity of the architecture is determined by considering winding errors, represented by uncertainties in the independent variables $\{t_i, p_i, q_i\}$.

It is straightforward to see that a coil with an even number of layers, all layers wrapping the same length of fiber and all layers extending from the bottom to the top of the drum will yield a null pointing error due to a linear longitudinal index gradient. This is the ideal geometry of the fiber optic coils considered here. Given L , N , p_1 , R_1 and q_i , the project equations for this coil are, together with Equation (8):

$$L_i = L/N, \quad (10a)$$

$$z_0 = \frac{p_1 L}{2\pi N \sqrt{R_1^2 + p_1^2}}, \quad (10b)$$

$$p_i = \frac{R_1}{\sqrt{[L/(\pi z_0 N)]^2 - 1}}, \quad (10c)$$

$$t_i = z_0/p_i, \quad (10d)$$

where p_1 and q_i should all be greater or equal to the fiber diameter D , and usually the drum length l_D is related to z_0 by $l_D = z_0 + D$. In this case, the pointing error due to a linear longitudinal index gradient can be written, independently of the radial architecture:

$$\theta_z = \frac{n_0 n_z L^2}{48 A N^2} [1 - (-1)^N], \quad (11)$$

In the same way, the pointing error due to a linear radial index gradient can be made null for coils comprising almost any number of layers by a suitable choice of architecture.

To explain coil architectures, it is necessary to consider an unwound fiber and designate distinctly the layers coiled by each half of the fiber, for example, as layer type 0 if it is wound from the left end and type 1 if from the right. Straight winding, or monopole, which coils just one end of the fiber layer after layer, is represented by a layer sequence of 1111... or, equivalently, 0000.... Dipole winding begins from the middle of the fiber and turns both ends in alternation, yielding the layer sequence 101010...; quadrupole [6] repeats the period 1001, yielding the sequence 10011001..., as shown in Fig. 1; and one interesting octupole winding architecture repeats the eight layer sequence 10010110. If the number of layers is larger than four it may useful to represent the layer sequence by hexadecimal numbers, with each of the hexadecimal digits representing four layers (the first digit may represent less than four): a

twelve layer quadrupole coil is represented by 999 and a sixteen layer octupole coil by 9696. This representation is used to describe the different architectures studied.

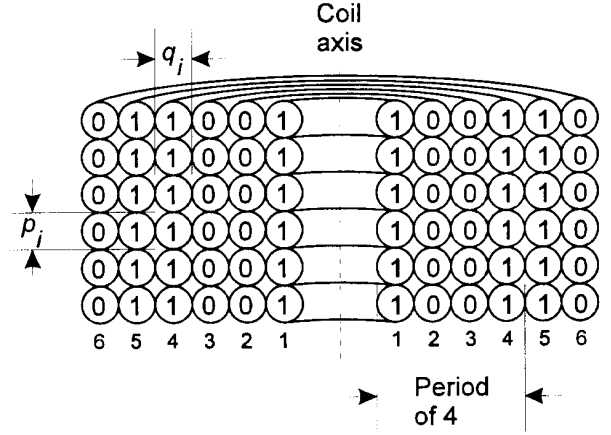


Figure 1. Quadrupole coil architecture. Each layer is identified by its order from the inside of the coil and a binary 0 or 1, being one half of the coil length represented by 1 and the other half by 0.

For architectures with a number N of layers from 1 to 32, one set of layer sequences that zero or minimize the radial pointing error is represented in hexadecimal digits by 1, 2, 5, 9, 11, 29, 56, 96, 169, 269, 499, A99, 1196, 2699, 5966, 9966, 16699, 26699, 49996, A6999, 119966, 266999, 599666, 999666, 1666999, 2666999, 4999966, A669999, 11999666, 26669999, 59996666. For these, the pointing error as calculated by Equations (5) and (6) is of the form

$$\theta_r = 2\theta_0, \text{ if } N = 3 \text{ or } N = 4,$$

$$\theta_r = \theta_0 (-1)^{k+1} \delta_{N,4k-2}, \text{ otherwise, } k = 0, 1, 2, \dots, \quad (12)$$

where

$$\theta_0 = \frac{n_0 n_r L^2}{4 A N^2 (N - 1)}, \quad (13)$$

and $\delta_{mn} = 1$ if $m = n$ and 0 otherwise. This set of architectures is chosen to yield the least pointing error given the number of layers, keeping the same length of fiber and the same longitudinal extension in each layer. It can be shown that, for an ideal geometry of the coil, the error due to a linear radial index gradient cannot be zero if the number of layers is $4k + 2$, $k = 0, 1/4, 1/2, 3, \dots$. Also, for $N \geq 8$, there are several different solutions that zero the error, yielding the same minimum pointing errors given by Equation (12). The set can be easily extended to any number of layers by induction.

To demonstrate the improvement of the proposed architectures over others, plots of the radial pointing error are shown in Fig. 2. Other architectures have

an increasing or an oscillating with increasing amplitude error as the number of layers increases, whereas the proposed architectures have a constant null error for most cases.

Besides its magnitude, the sensitivity of the pointing error to winding uncertainties is also important. This can be determined by the calculation of the error propagation formulae:

$$\Delta\theta_E = \Delta\theta_r + \Delta\theta_z, \quad (14a)$$

$$\Delta\theta_{r,z} = \sqrt{\sum_{i=1}^N \left[\left(\frac{\partial\theta_{r,z}}{\partial L_i} \Delta L_i \right)^2 + \frac{\partial\theta_{r,z}}{\partial(t_i p_i)} \Delta(t_i p_i) \right]^2}, \quad (14b)$$

where the partial derivatives are calculated for $L_i = L/N$ and $t_i p_i = z_0$, all i . ΔL_i can be computed from (7) and (8) and the same algorithm in terms of the winding errors Δt_i , Δp_i and Δq_i . Plots of $\Delta\theta_r$ are shown in Fig. 3, illustrating that the proposed set has the lowest sensitivity. The sensitivity $\Delta\theta_z$ is independent of the radial architecture of the coil.

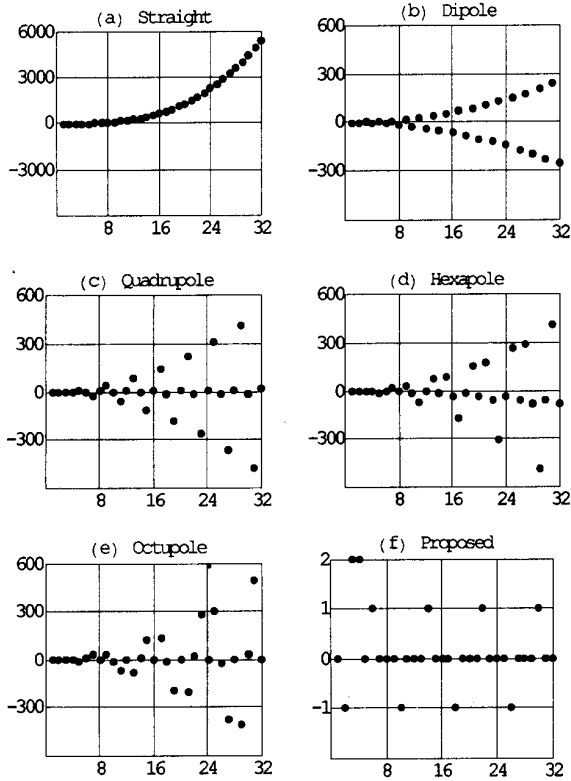


Figure 2. Pointing errors due to a linear radial index gradient (θ_r) for different coil architectures, as a function of the number of layers. Vertical scale in units of θ_0 , as defined by Eq. (13). a) Straight winding (1111...); b) dipole (1010...); c) quadrupole (1001...); d) hexapole (101001...); e) octupole (10010110...) and f) the proposed sequence of architectures.

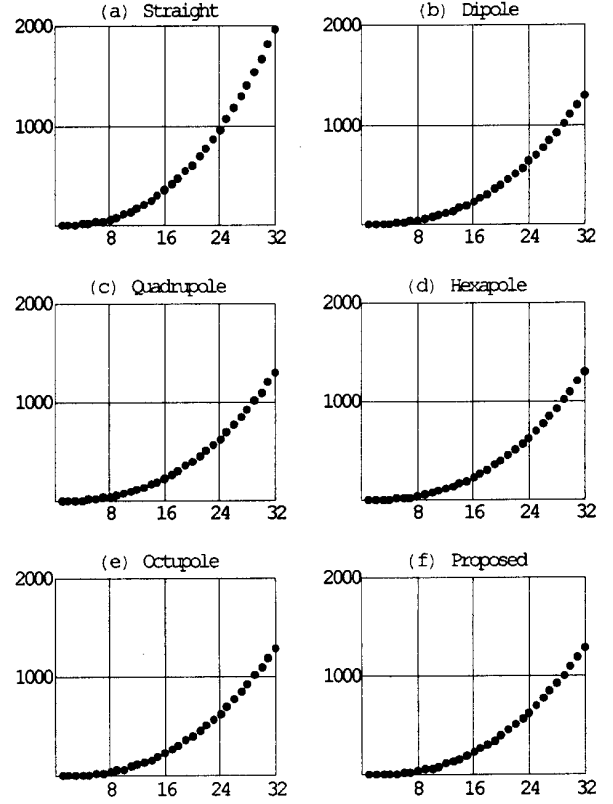


Figure 3. Sensitivity of pointing errors due to a linear radial index gradient ($\Delta\theta_r$), for different coil architectures, as a function of the number of layers. Vertical scale in units of $\theta_0 \Delta L_i / L_i$, where ΔL_i is the uncertainty of the layer fiber length, assumed constant, and θ_0 is given by Eq. (13). a) Straight winding (1111...); b) dipole (1010...); c) quadrupole (1001...); d) hexapole (101001...); e) octupole (10010110...) and f) the proposed sequence of architectures.

In the set of architectures proposed, whenever a segment of 9's and 6's is present together, their order can be interchanged at random (provided that a segment 6 is not placed the beginning of the sequence) without altering the pointing error or its sensitivity to the fiber length L_i of any layer. Thus, for example, the segment 9966 can be exchanged by 9669 or 9696, and a 32 layer octupole coil 96969696 is completely equivalent to a coil with sequence 99996666. This latter has advantages over the former for requiring a simpler winding process.

As layer is wound over layer, it may become necessary to add a spacer after a number of layers to even out the drum surface for the next layer. For any of the proposed architectures, a spacer at every fourth or eighth layer will not alter the pointing error of sequences beginning with 9, A and 11, but the sensitivity to L_i of the radial part of the pointing error is altered.

IV Experiment

A machine was designed and built to perform the winding of any architecture, as presented in Fig. 4. The rotation of the drum to wind fiber and the helical step p are controlled by computer. Delivering spools, each containing half of the fiber, are mounted on low friction bearings with their axes perpendicular to the drum axis. When feeding, they are kept on a horizontal plane to avoid spurious moments caused by mass unbalance on the spools, which can induce variations on the fiber tension. Winding tension can be adjusted to below 5 mN by a braking system based on the friction of a tensioned 0.40 mm diameter copper wire on a 33 mm diameter aluminum drum attached to the delivering spool.

A 32 layer coil using the octupole 96969696 architecture was wound on a 10 cm diameter drum. The fiber diameter was (0.198 ± 0.004) mm and the longitudinal helical pitch was adjusted to be (0.20 ± 0.01) mm per turn. No interstitial filler was used but a (0.100 ± 0.002) mm thick acetate film every eighth layer to even out the drum for the next layers. The numbers of turns in each layer were $\{106.7, 106.0, 103.0, 105.5, 101.0, 100.0, 102.0, 101.0, 106.0, 103.9, 106.0, 102.0, 93.9, 103.2, 106.0, 102.0, 91.8, 103.3, 87.3, 94.9, 104.8, 106.1, 102.0, 104.0, 102.0, 103.0, 101.6, 95.0, 92.5, 87.2, 93.7, 92.1\}$, with uncertainties of ± 0.1 turn. The layer radius and length of fiber were not controlled in this coil. The fiber tension was kept below 50 mN by using a mass of 160 g applying a tension of about 1.60 N on the copper wire of the spool braking system. For linear radial and longitudinal gradients of total difference of n_r and n_z , respectively, the pointing error is predicted to be, in radians,

$$\theta_E = (1.1 \pm 0.2) \cdot 10^2 n_r \pm 2.3 \cdot 10^4 n_z. \quad (16)$$

This preliminary experiment with optical fiber winding techniques has shown the feasibility of keeping the winding errors below 1% with a very simple automatic winding process. The machine devised for this process being a first approach, some improvements on it can be readily performed and are recommended.

Final characterization of the assembled coils will be carried out by realizing a Sagnac interferometer and measuring the noise and drift of the Sagnac phase under several environments. For the internal quality of the coil, the degradation of polarization conservation, caused mainly by localized perturbations, such as microbending and stress, will be tested with optical coherence domain polarimetry [8].

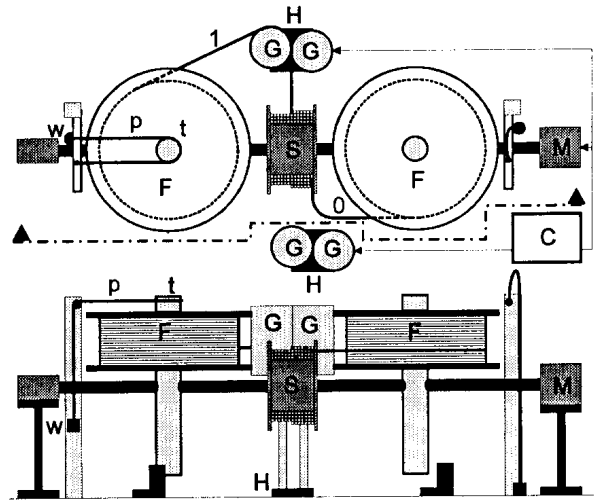


Figure 4. Programmable winding station, showing one top view (top) and one side view (bottom). 1: first half of the optical fiber; 0: second half of the optical fiber; F: feeding spools; p: copper wire; t: friction-based tension controller; w: weight; G: fiber guide; S: coil spool; C: computer, for motion control; H: precision motorized horizontal translation stage; M: precision reversible rotation motor.

V Conclusions

A fundamental device in the interferometric fiber optic gyroscope is the fiber coil itself, which should be designed to maximize its sensitivity to inertial rotation and minimize its sensitivity to any other environmental perturbation. One parameter to measure the suitability of a coil to rotation sensing is the calculated pointing error due to linear gradients of perturbation in the refractive index of the fiber. This parameter can be reduced by symmetrical winding, beginning from the middle of the fiber and winding both half-ends in alternation. Using this principle, several symmetrical coil architectures are proposed, examined and compared. Different architectures, devised to minimize or zero the pointing error, comprise a sequence of layers wound in a helical curve, each layer identified by its order from the inside of the coil and a binary 0 or 1 accordingly to the half-end of the fiber. Thus an architecture with several layers can be described by a hexadecimal number, each digit representing four layers. Using this representation, the set of architectures studied for 1 to 32 layer coils is: 1, 2, 5, 9, 11, 29, 56, 96, 169, 269, 499, A99, 1196, 2699, 5966, 9966, 16699, 26699, 49996, A6999, 119966, 266999, 599666, 999666, 1666999, 2666999, 4999966, A669999, 11999666, 26669999, 59996666, 99996666. This set can be easily extended following the repeating pattern with period of 8. All these architectures zero the pointing

error due to a radial linear gradient of refractive index, except the ones with $4k + 2$ layers, $k = 0, 1/4, 1/2, 1, 2, 3, \dots$; and all with an even number of layers zero the pointing error due to a longitudinal linear index gradient. Project equations are derived and sensitivity of the pointing error to winding errors for all proposed architectures are shown to be low and stable. All basic elements are given for the design of fiber optic coils for almost any kind of gyroscope.

To assembly these coils in practice, a programmable machine is devised and built to wind the fiber with an adjustable low tension in any of the proposed architectures. A first loop is wound for a fiber optic gyroscope prototype and is under experimental characterization. The feasibility of keeping the winding errors below 1% with this simple automatic winding process is demonstrated.

VI Acknowledgements

This work was funded by the Brazilian Air Ministry.

References

- 1 Michael S. Perlmutter, Christopher I. Reynolds and Ram Yahalom. "Initial Production Results of a New Family of Fiber Optic Gyroscopes". In: H. Sorg (ed.), *Symposium Gyro Technology 1997*, pages 6.1- 6.11. Stuttgart, September 1997.
- 2 W. K. Burns. "Fiber Optic Gyroscopes - Light is Better". *Optics & Photonics News*, **9**(5), 28 (1998).
- 3 V. Vali and R. W. Shorthill, "Fiber Ring Interferometer". *Applied Optics*, **15**(5), 1099 (1976).
- 4 A. R. Mickelson, N. R. Basavanhally and Y. C. Lee (Ed.), *Optoelectronic Packaging*, John Wiley & Sons Inc., (Wiley series in microwave and optical engineering), New York, 1997.
- 5 D. M. Shupe, "Thermally induced nonreciprocity in the fiber-optic interferometer". *Applied Optics*, **19** (5), 654 (1980).
- 6 Nicholas J. Frigo, "Compensation of Linear Sources of Non-Reciprocities in Sagnac Interferometers". *Fiber Optic and Laser Sensors I*, Proc. SPIE vol. 412, 1983, pages 268-271.
- 7 G. Sagnac, "L'éther lumineux démontré par l'effet du vent relatif d'éther dans un interféromètre en rotation uniforme". *C. R. Acad. Sci.* **95**, 708 (1913).
- 8 Hervé Lefèvre, *The Fiber-Optic Gyroscope*, Artech House Boston 1993, Chapter 5.

1 Michael S. Perlmutter, Christopher I. Reynolds and